

Note added after first publication:

28th January 2019 This ESI replaces that originally uploaded on 13th March 2018 in which an incorrect CCDC number was given.

Supporting Information

Multiple Cluster CH Activations and Transformations of Furan by Triosmium Carbonyl Complexes

Richard D. Adams*, Joseph Kiprotich and Mark D. Smith

General Data.

All reactions were performed under a nitrogen atmosphere by using the standard Schlenk techniques. Reagent grade solvents were dried by the standard procedures and were freshly distilled prior to use. Infrared spectra were recorded on a Thermo Fisher Scientific Nicolet IS10 FT-IR spectrophotometer. ¹H NMR spectra were recorded on a Varian Mercury 300 spectrometer operating at 300.1 MHz. Mass spectrometric (MS) measurements performed by a direct-exposure probe by using electron impact ionization (EI) were made on a VG 70S instrument. Os₃(CO)₁₀(NCMe)₂^[1] was prepared according to a previously reported procedure. Product separations were performed by TLC in the open air on Analtech 0.25 and 0.5 mm silica gel 60 Å F₂₅₄ glass plates. CCDC 1822078-1822082 and 1836227 contain the supplementary crystallographic data for this paper. These data can be obtained free of charge via www.ccdc.cam.ac.uk/conts/retrieving.html (or from the Cambridge Crystallographic Data Centre, 12, Union Road, Cambridge CB21EZ, UK; fax: (+ 44)1223-336-033; or deposit@ccdc.cam.ac.uk).

Syntheses of Os₃(CO)₁₀(μ-η²-C₄H₃O)(μ-H), and Os₃(CO)₉(μ₃, η²-C₄H₂O)(μ-H)₂, 1

Os₃(CO)₁₀(μ-η²-C₄H₃O)(μ-H) was prepared by using a modified procedure of Himmelreich and Muller.^[2] 2.0 mL of furan was added to a 10 mL high pressure glass vessel with 42.0 mg of Os₃(CO)₁₀(NCMe)₂ (0.045 mmol). The mixture was then heated at 80 °C in a sealed high-pressure reactor for 2 h. The excess furan was removed *in vacuo*, and the orange solid

Note added after first publication:

28th January 2019 This ESI replaces that originally uploaded on 13th March 2018 in which an incorrect CCDC number was given.

separated by TLC in silica gel. Elution with pure hexane yielded 29.0 mg of $\text{Os}_3(\text{CO})_{10}(\mu, \eta^2\text{-C}_4\text{H}_3\text{O})(\mu\text{-H})$, (70 % yield) and 3.7 mg of $\text{Os}_3(\text{CO})_9(\mu_3, \eta^2\text{-C}_4\text{H}_2\text{O})(\mu\text{-H})_2$, **1** (9 % yield). Compound **1** was subsequently obtained in a higher yield from $\text{Os}_3(\text{CO})_{10}(\mu, \eta^2\text{-C}_4\text{H}_3\text{O})(\mu\text{-H})$ by heating 36.0 mg it to reflux in 20 mL of octane for 1.5 h. 34.0 mg (99 % yield) of **1** was obtained. Spectral data for **1**: IR (ν_{CO} , cm^{-1} , in hexane): 2113 (s), 2085 (vs), 2060 (vs), 2036 (vs), 2030 (sh), 2014 (vs), 2002 (vs), 1989 (s), 1960 (w). ^1H NMR (in CD_2Cl_2): δ = 7.60 ppm (d, 1H, CH), 6.84 (d, 1H, CH), -19.54 (s, hydride, 2H). EI/MS m/z , 892 = M^+ .

Reaction of $\text{Os}_3(\text{CO})_{10}(\mu_3\text{-}\eta^2\text{-C}_4\text{H}_2\text{O})(\mu\text{-H})_2$, **1 with $\text{Os}_3(\text{CO})_{10}(\text{NCMe})_2$**

To a solution of 30.0 mg (0.034 mmol) of **1** in cyclohexane was added 61.0 mg (0.065 mmol) of $\text{Os}_3(\text{CO})_{10}(\text{NCMe})_2$ (added over 4h). The mixture was then heated to reflux with intermittent monitoring by IR for 4 h. The solvent was then removed *in vacuo* and the products were separated by TLC by using hexane solvent. This yielded in order of elution: 25.8 mg of $(\mu\text{-H})_2\text{Os}_3(\text{CO})_9(\mu_3\text{-}\eta^2\text{-2,3-}, \mu\text{-}\eta^2\text{-4,5-C}_4\text{HO})\text{Os}_3(\text{CO})_{10}(\mu\text{-H})$, **2** (63 % yield), 4.3 mg of $(\mu\text{-H})_2\text{Os}_3(\text{CO})_9(\mu_3\text{-}\eta^2\text{-2,3-}, \mu_3\text{-}\eta^2\text{-4,5-C}_4\text{O})\text{Os}_3(\text{CO})_9(\mu\text{-H})_2$, **3** (11 % yield), 5.2 mg of $(\mu\text{-H})_2\text{Os}_3(\text{CO})_9(\mu_3\text{-}\eta^1\text{-C-C-C-}\mu_3\text{-}\eta^1)\text{Os}_3(\text{CO})_9(\mu\text{-H})_2$, **4** (13 % yield) and 9.2 mg of **1** (unreacted). Spectral data for **2**: IR (ν_{CO} , cm^{-1} , in hexane): 2116 (w), 2103 (m), 2089 (s), 2069 (vs), 2066 (s), 2056 (m), 2040 (m), 2034 (vw), 2023 (sh), 2020 (s), 2009 (vw), 2002 (s), 1983 (vw). ^1H NMR (in CD_2Cl_2): δ = 7.57 ppm (s, 1H, CH), -15.83 (s hydride, 3H), VT- ^1H NMR (in CD_2Cl_2 , -50° C): δ = -15.95 ppm (s, hydride, 1H) -17.60 (s, hydride, 1H), -21.68 (s, hydride, 1H). EI/MS m/z , 1742 = M^+ . The isotopic distribution is consistent with the presence of six osmium atoms. Spectral data for **3**: IR (ν_{CO} , cm^{-1} , in hexane): 2118 (w), 2110 (vw), 2106 (m), 2088 (vs), 2083 (s), 2065 (vs), 2035 (s), 2022 (m), 2016 (vs), 2004 (vs), 1990 (w), 1972 (vw), 1964 (vw). ^1H NMR (in CD_2Cl_2): δ = -19.50 ppm (br, hydride, 4H). Low temp. ^1H NMR (in CD_2Cl_2 , -90° C): δ = -17.51 ppm (s,

Note added after first publication:

28th January 2019 This ESI replaces that originally uploaded on 13th March 2018 in which an incorrect CCDC number was given.

hydride, 2H), -21.71 (s, hydride, 2H). EI/MS m/z , 1714 = M^+ . The isotopic distribution is consistent with the presence of six osmium atoms. Spectral data for **4**: IR (ν_{CO} , cm^{-1} , in hexane): 2114 (vw), 2101 (s), 2084 (m), 2080 (vs), 2068 (vw), 2062 (s), 2056 (m) 2036 (w), 2026 (s), 2014 (vs), 2009 (s), 1997 (w), 1989 (vw), 1981 (w). 1H NMR (in CD_2Cl_2): δ = -19.56 ppm (s, hydride, 4H), LT- 1H NMR (in CD_2Cl_2 , -90° C): δ = -19.78 (br, hydride, 4H). EI/MS m/z , 1686 = M^+ . The isotopic distribution is consistent with the presence of six osmium atoms.

Decarbonylation of $Os_3(CO)_9(\mu-H)_2(\mu_3-\eta^2-2,3-\mu-\eta^2-4,5-C_4HO)Os_3(CO)_{10}(\mu-H)$, **2**

27.0 mg (0.016 mmol) of compound **2** was dissolved in heptane and heated under reflux for 5 hours with intermittent monitoring by IR. The solvent was then removed *in vacuo* and the products were isolated by TLC by using hexane solvent. This yielded in order of elution: 2.2 mg of $(\mu-H)_3Os_3(CO)_9(\mu_3-C=C=C-\mu_2)Os_3(CO)_{10}(\mu-H)$, **5** (8 % yield), 2.6 mg of compound **3** (9.5 % yield), 2.7 mg of compound **4** (9.5 % yield) and 0.7 mg of $(\mu-H)Os_3(CO)_9(\mu_3-\eta^2-CH-C-CH-C=O-\mu_2-\eta^2)Os_3(CO)_{10}(\mu-H)$, **6** (2.5% yield).

Spectral data for **5**: IR (ν_{CO} , cm^{-1} , in hexane): 2120 (vw), 2094 (vs), 2087 (sh), 2077 (w), 2062 (s), 2053 (m), 2034 (s), 2023 (w), 2015 (vs), 2006 (s), 1992 (m), 1983 (vw), 1976 (w), 1900 (m, br) 1H NMR (in CD_2Cl_2): δ = -15.79 ppm (s hydride, H), -18.93 (s hydride, 3H). EI/MS m/z , 1714 = M^+ . The isotopic distribution is consistent with the presence of six osmium atoms.

Spectral data for **6**: IR (ν_{CO} , cm^{-1} , in hexane): 2111 (vw), 2101 (s), 2077 (vs), 2072 (m), 2058 (m), 2050 (s), 2032 (w), 2029 (s), 2014 (vs), 2007 (w), 2000 (m), 1987 (w), 1987 (m), 1982 (w) 1H NMR (in CD_2Cl_2): δ = 9.13 (s, CH), 3.87 (s, CH), -13.81 (s, hydride), -22.10 (s, hydride). EI/MS m/z , 1742 = M^+ . The isotopic distribution is consistent with the presence of six osmium atoms.

Conversion of compound **3 to compounds **5** and **4****

Note added after first publication:

28th January 2019 This ESI replaces that originally uploaded on 13th March 2018 in which an incorrect CCDC number was given.

4.7 mg (0.003 mmol) of **3** was dissolved in toluene- d_8 in an NMR tube and heated at 80 °C for 75 h with intermittent monitoring by NMR. The products were then isolated by TLC on silica using hexane solvent as eluent. In order of elution 3.7 mg of **5** (79 % yield) and 0.4 mg of **4** (9 % yield) were obtained.

Conversion of compound 5 to compound 4

10.1 mg (0.006 mmol) of **5** was dissolved in toluene- d_8 in an NMR tube and heated at 105 °C for a period of 10 days with intermittent monitoring by NMR. The products were then isolated by TLC on silica using hexane as the eluent to obtain 7.3 mg of compound **4** (74 % yield).

Conversion of compound 6 to compounds 4 and 5

A sample of **6** in toluene- d_8 solution was heated to 105 °C for 24 h. The sample was monitored by ¹H NMR spectroscopy which showed the formation of equal amounts of compounds **4** and **5** were formed after this period.

Crystallographic Analyses

Yellow single crystals of **1**, **2**, **3** and **4** were obtained by slow evaporation of solvent from solutions of each of the compounds in hexane solvent. Single crystals of red **5** and yellow **6** suitable for x-ray diffraction analyses were obtained by slow evaporation of solvent from solutions in hexane/methylene chloride solvent mixtures. Crystal **1** was glued onto the end of a thin glass fiber and X-ray intensity data measured by using a Bruker SMART APEX CCD-based diffractometer by using Mo K α radiation ($\lambda = 0.71073$ Å). The raw data frames were integrated with the SAINT⁺ program by using a narrow-frame integration algorithm.^[3] Correction for Lorentz and polarization effects were also applied with SAINT⁺. An empirical absorption correction based on the multiple measurements of equivalent reflections was applied using the program SADABS in each analysis.

Note added after first publication:

28th January 2019 This ESI replaces that originally uploaded on 13th March 2018 in which an incorrect CCDC number was given.

It was solved by a combination of direct methods and difference Fourier syntheses and refined by full-matrix least-squares on F^2 by using the SHELXTL software package.^[4] X-ray intensity data for crystals **2-6** were collected at 100(2) K using a Bruker D8 QUEST diffractometer equipped with a PHOTON-100 CMOS area detector and an Incoatec Microfocus source (Mo $K\alpha$ radiation, $\lambda = 0.71073 \text{ \AA}$).^[5]

Compound 2: The data collection strategy consisted of five 180° ω -scans at different ϕ settings, using a scan width per image of 0.5° . The crystal-to-detector distance was 5.0 cm and each image was measured for 6 s with the detector operated in shutterless mode. The average reflection redundancy was 5.5. The raw area detector data frames were reduced, scaled and corrected for absorption effects using the SAINT^[5] and SADABS^[6] programs. Final unit cell parameters were determined by least-squares refinement of 9796 reflections in the range $4.767^\circ \leq 2\theta \leq 55.228^\circ$ taken from the data set. All non-hydrogen atoms were refined with anisotropic displacement parameters. Hydrogen atoms on the furan ring were placed in geometrically idealized positions and were included as standard riding atoms during the least-squares refinements.

Compound 3: The data collection strategy consisted of five 180° ω -scans each at a different ϕ setting, with a scan width per image of 0.6° . The crystal-to-detector distance was 4.5 cm and each image was measured for 4 s with the detector operated in shutterless mode. The average reflection redundancy was 6.1. The raw area detector data frames were reduced, scaled and corrected for absorption effects using the SAINT and SADABS. Final unit cell parameters were determined by least-squares refinement of 9802 reflections in the range $4.938^\circ \leq 2\theta \leq 55.405^\circ$ taken from the data set.

Compound 4: The data collection strategy consisted of five 180° ω -scans at different ϕ settings and one 360° ϕ -scan, with a scan width per image of 0.5° . The crystal-to-detector distance was 5.0

Note added after first publication:

28th January 2019 This ESI replaces that originally uploaded on 13th March 2018 in which an incorrect CCDC number was given.

cm and each image was measured for 5 s with the detector operated in shutterless mode. The average reflection redundancy was 6.8. The raw area detector data frames were reduced, scaled and corrected for absorption effects using the SAINT and SADABS programs. Final unit cell parameters were determined by least-squares refinement of 9901 reflections in the range $4.993^\circ \leq 2\theta \leq 59.946^\circ$ taken from the data set.

Compound **5**: Crystals formed as red plates which visibly exhibited lamellar twinning and poor extinctions in polarized light. Several crystals examined, intact or cleaved and of various sizes, persistently gave closely paired or split diffraction spots, along with difficulty in indexing the diffraction pattern to a single reasonable unit cell. Eventually it was determined that crystals of the material are twinned by non-merohedry. Using the Bruker Cell Now program,^[7] a set of 1215 reflections from the data set were indexed entirely to two domains with the reported primitive monoclinic unit cell parameters. The derived twin law, relating indices of one domain to those of the other, is (1 0 0 / 0 -1 0 / -0.74 0 -1). The twin law corresponds to a 180° rotation about the reciprocal-space [100] axis. The raw area detector data frames were reduced and corrected for absorption effects using the SAINT⁺ and TWINABS programs.^[8] TWINABS also constructed SHELX HKLF-4 and HKLF-5 format reflection files for solution and refinement, respectively. Final unit cell parameters were determined by least-squares refinement of 5913 reflections in the range $4.756^\circ < 2\theta < 56.908^\circ$ taken from both twin domains of the crystal. The structure was solved by dual-space methods with SHELXT.^[9] Subsequent difference Fourier calculations and full-matrix least-squares twin refinement against F^2 were performed with SHELXL-2017^[10] using OLEX2.^[11] The major twin domain volume fraction refined to 0.804(1).

Compound **6**: The data collection strategy consisted of four 180° ω -scans at different ϕ settings and two 360° ϕ -scans at different ω angles, with a scan width per image of 0.5°. The crystal-to-

Note added after first publication:

28th January 2019 This ESI replaces that originally uploaded on 13th March 2018 in which an incorrect CCDC number was given.

detector distance was 5.0 cm and each image was measured for 5 s with the detector operated in shutterless mode. The average reflection redundancy was 14.0. The raw area detector data frames were reduced, scaled and corrected for absorption effects using the SAINT and SADABS programs. Final unit cell parameters were determined by least-squares refinement of 9704 reflections in the range $4.593^{\circ} \leq 2\theta \leq 56.450^{\circ}$ taken from the data set.

Crystal data, data collection parameters, and results of the analyses are listed in Tables 1 and 3.

Compounds **1** - **4** crystallized in the triclinic crystal system while **5** and **6** crystallized in the monoclinic crystal system. The space group *P*-1 was assumed for **1** - **4** and was confirmed by the successful solution and refinement of the structures. For compound **6**, the space group *P*2₁/c was indicated by the systematic absences in the data and confirmed by the successful solution and refinement of the structures. Compound **5** crystallized in the space group *P*2₁/*n* of the monoclinic system. The asymmetric unit consisted of one independent molecule. All non-hydrogen atoms in all the compounds were refined with anisotropic displacement parameters. Reasonable hydride atom positions for all compounds were obtained from difference Fourier maps and refined. The bridging hydride ligands that could not be refined freely were restrained with distance constraints of 1.80 Å and the hydride displacement parameters were treated as riding on the parent Os atoms. Crystal data, data collection parameters, and results of the analyses are listed in Tables 1 and 2.

Note added after first publication:

28th January 2019 This ESI replaces that originally uploaded on 13th March 2018 in which an incorrect CCDC number was given.

Table 1. Crystallographic Data for Compounds **1**, **2** and **3**

Compound	1	2	3
Empirical formula	Os ₃ O ₁₀ C ₁₃ H ₄	Os ₆ O ₂₀ C ₂₃ H ₄	Os ₆ O ₁₉ C ₂₂ H ₄
Formula weight	890.76	1741.46	1713.45
Crystal system	Triclinic	Triclinic	Triclinic
Lattice parameters			
<i>a</i> (Å)	8.6127(4)	11.3105(5)	9.7044(5)
<i>b</i> (Å)	9.0730(4)	16.1718(8)	11.2944(5)
<i>c</i> (Å)	12.9331(6)	18.3462(8)	15.7359(7)
α (deg)	79.015(1)	87.0138(14)	82.9237(16)
β (deg)	79.938(1)	89.5808(15)	86.2639(16)
γ (deg)	63.360(1)	81.0114(15)	67.6042(15)
<i>V</i> (Å ³)	2403.4(5)	3310.0(3)	1582.19(13)
Space group	<i>P</i> -1	<i>P</i> -1	<i>P</i> -1
<i>Z</i> value	2	4	2
ρ_{calc} (g/cm ³)	3.229	3.495	3.597
μ (Mo K α) (mm ⁻¹)	20.800	23.023	24.077
Temperature (K)	294(2)	100(2)	100(2)
2 θ max (°)	56.56	55.26	55.5
No. Obs. (<i>I</i> > 2 σ (<i>I</i>))	3982	12620	6142
No. Parameters	242	899	432
Goodness of fit (GOF)	1.035	1.064	1.066
Max. shift in cycle	0.001	0.001	0.001
Residuals*: R1; wR2	0.0386; 0.1073	0.0316; 0.0599	0.0294, 0.0467
Absorption Correction	multi-scan	multi-scan	multi-scan
Max/min	1.00/0.164	0.6560/0.1687	0.1515/0.0615
Largest peak in Final Diff.	1.855	2.483	2.34
Map (e ⁻ /Å ³)			

*R1 = $\sum_{\text{hkl}} (|F_{\text{obs}}| - |F_{\text{calc}}|) / \sum_{\text{hkl}} |F_{\text{obs}}|$; wR2 = $[\sum_{\text{hkl}} w(|F_{\text{obs}}| - |F_{\text{calc}}|)^2 / \sum_{\text{hkl}} w F_{\text{obs}}^2]^{1/2}$; $w = 1/\sigma^2(F_{\text{obs}})$; GOF = $[\sum_{\text{hkl}} w(|F_{\text{obs}}| - |F_{\text{calc}}|)^2 / (n_{\text{data}} - n_{\text{vari}})]^{1/2}$.

Note added after first publication:

28th January 2019 This ESI replaces that originally uploaded on 13th March 2018 in which an incorrect CCDC number was given.

Table 2. Crystallographic Data for Compounds **4**, **5** and **6**

Compound	4	5	6
Empirical formula	Os ₆ O ₁₈ C ₂₁ H ₄	Os ₆ O ₁₉ C ₂₂ H ₄	Os ₆ O ₂₀ C ₂₃ H ₄
Formula weight	1685.44	1713.45	1741.46
Crystal system	Triclinic	Monoclinic	Monoclinic
Lattice parameters			
<i>a</i> (Å)	9.4304(5)	15.0941(12)	14.0260(7)
<i>b</i> (Å)	9.4911(5)	9.2362(7)	9.5121(5)
<i>c</i> (Å)	20.1170(9)	23.5146(18)	24.6707(13)
α (deg)	98.507(2)	90.00	90.00
β (deg)	95.159(2)	103.717(2)	96.081(2)
γ (deg)	119.294(1)	90.00	90.00
<i>V</i> (Å ³)	1525.29(13)	3184.7(4)	3273.0(3)
Space group	<i>P</i> -1	<i>P</i> 2 ₁ /n	<i>P</i> 2 ₁ /c
<i>Z</i> value	2	4	4
ρ_{calc} (g/cm ³)	3.670	3.574	3.534
μ (Mo K α) (mm ⁻¹)	24.970	23.923	23.284
Temperature (K)	100(2)	100(2)	100(2)
2 θ max (°)	59.94	57.0	56.450
No. Obs. (<i>I</i> > 2 σ (<i>I</i>))	7153	6923	6804
No. Parameters	422	439	450
Goodness of fit (GOF)	1.081	1.080	1.059
Max. shift in cycle	0.003	0.001	0.001
Residuals*: R1; wR2	0.0306, 0.0434	0.0414, 0.0953	0.0291, 0.0512
Absorption Correction,	multi-scan	multi-scan	multi-scan
Max/min	0.1723/0.3576	0.6462/0.0867	0.1688/0.0787
Largest peak in Final Diff.	1.771	2.348	2.421
Map (e ⁻ /Å ³)			

*R1 = $\sum_{\text{hkl}} (|F_{\text{obs}}| - |F_{\text{calc}}|) / \sum_{\text{hkl}} |F_{\text{obs}}|$; wR2 = $[\sum_{\text{hkl}} w(|F_{\text{obs}}| - |F_{\text{calc}}|)^2 / \sum_{\text{hkl}} w F_{\text{obs}}^2]^{1/2}$; w = $1/\sigma^2(F_{\text{obs}})$; GOF = $[\sum_{\text{hkl}} w(|F_{\text{obs}}| - |F_{\text{calc}}|)^2 / (n_{\text{data}} - n_{\text{vari}})]^{1/2}$.

Note added after first publication:

28th January 2019 This ESI replaces that originally uploaded on 13th March 2018 in which an incorrect CCDC number was given.

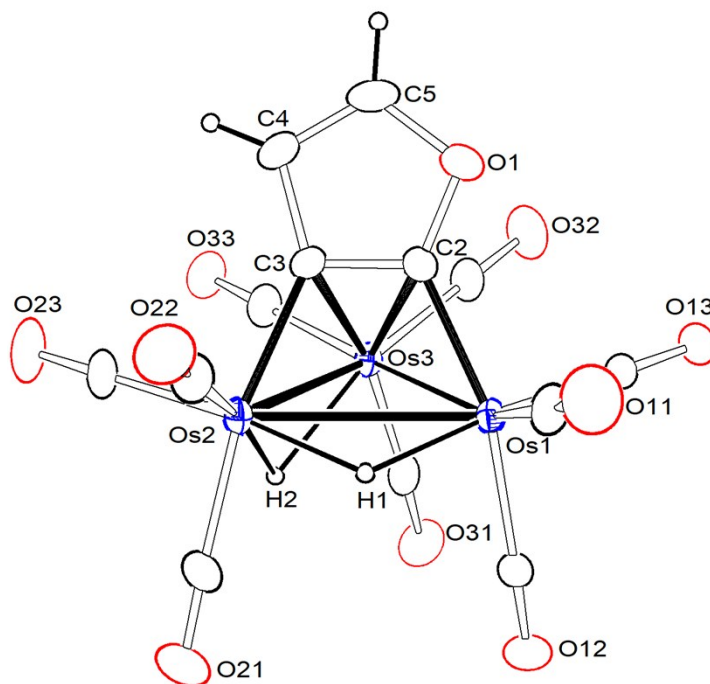


Figure 1. An ORTEP diagram of the molecular structure $\text{Os}_3(\text{CO})_9(\mu_3\text{-}\eta^2\text{-C}_4\text{H}_2\text{O})(\mu\text{-H})_2$, **1** showing 20% thermal ellipsoid probability. Selected interatomic bond distances (Å) are as follows: $\text{Os}(1) - \text{Os}(2) = 3.0811(4)$, $\text{Os}(1) - \text{Os}(3) = 2.7682(4)$, $\text{Os}(2) - \text{Os}(3) = 2.8558(4)$, $\text{Os}(1) - \text{C}(2) = 2.063(8)$, $\text{Os}(2) - \text{C}(3) = 2.117(8)$, $\text{Os}(3) - \text{C}(3) = 2.313(8)$, $\text{Os}(3) - \text{C}(2) = 2.394(8)$

Note added after first publication:

28th January 2019 This ESI replaces that originally uploaded on 13th March 2018 in which an incorrect CCDC number was given.

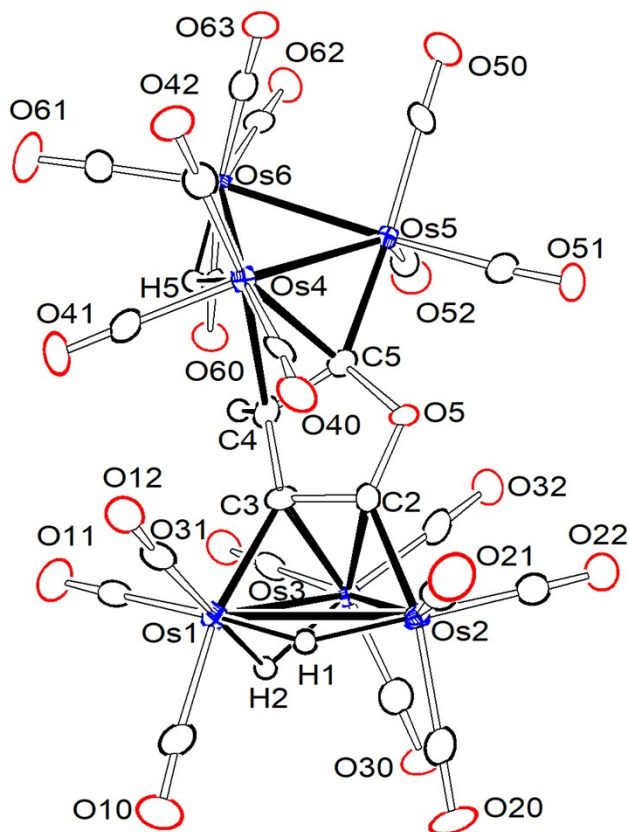


Figure 2. An ORTEP diagram of the molecular structure of $\text{Os}_3(\text{CO})_9(\mu\text{-H})_2(\mu_3\text{-}\eta^2\text{-2,3-}\mu\text{-}\eta^2\text{-4,5-C}_4\text{HO})\text{Os}_3(\text{CO})_{10}(\mu\text{-H})$, **2** showing 50% thermal ellipsoid probability. Selected interatomic bond distances (Å) are as follows: $\text{Os}(1) - \text{Os}(2) = 3.0814(5)$, $\text{Os}(1) - \text{Os}(3) = 2.8512(5)$, $\text{Os}(2) - \text{Os}(3) = 2.7811(5)$, $\text{Os}(1) - \text{C}(3) = 2.141(9)$, $\text{Os}(2) - \text{C}(2) = 2.031(9)$, $\text{Os}(3) - \text{C}(2) = 2.397(8)$, $\text{Os}(3) - \text{C}(3) = 2.245(8)$, $\text{Os}(5) - \text{C}(5) = 2.101(9)$, $\text{Os}(4) - \text{C}(5) = 2.346(9)$, $\text{Os}(4) - \text{C}(4) = 2.496(9)$

Note added after first publication:

28th January 2019 This ESI replaces that originally uploaded on 13th March 2018 in which an incorrect CCDC number was given.

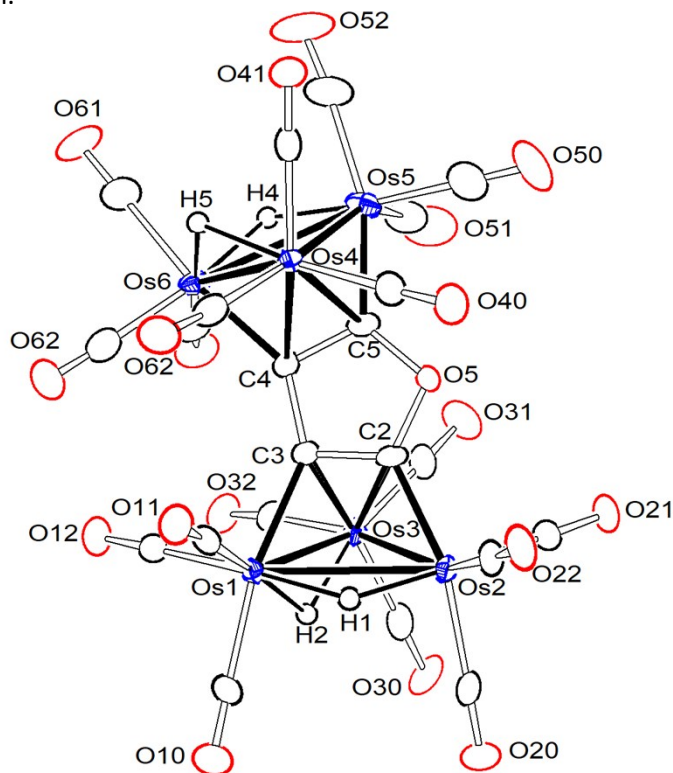


Figure 3. An ORTEP diagram of the molecular structure of $\text{Os}_3(\text{CO})_9(\mu\text{-H})_2(\mu_3\text{-}\eta^2\text{-}2,3\text{-}\mu_3\text{-}\eta^2\text{-}4,5\text{-C}_4\text{O})\text{Os}_3(\text{CO})_9(\mu\text{-H})_2$, **3** showing 50% thermal ellipsoid probability. Selected interatomic bond distances (\AA) are as follows: $\text{Os}(1) - \text{Os}(2) = 3.0695(4)$, $\text{Os}(1) - \text{Os}(3) = 2.8480(4)$, $\text{Os}(2) - \text{Os}(3) = 2.7782(4)$, $\text{Os}(1) - \text{C}(3) = 2.131(7)$, $\text{Os}(2) - \text{C}(2) = 2.040(7)$, $\text{Os}(3) - \text{C}(2) = 2.336(7)$, $\text{Os}(3) - \text{C}(3) = 2.310(7)$, $\text{Os}(5) - \text{C}(5) = 2.041(7)$, $\text{Os}(4) - \text{C}(5) = 2.325(7)$, $\text{Os}(4) - \text{C}(4) = 2.320(7)$, $\text{Os}(6) - \text{C}(4) = 2.131(7)$, $\text{C}(4) - \text{C}(5) = 1.415(10)$, $\text{C}(2) - \text{C}(3) = 1.392(10)$

28th January 2019 This ESI replaces that originally uploaded on 13th March 2018 in which an incorrect CCDC number was given.

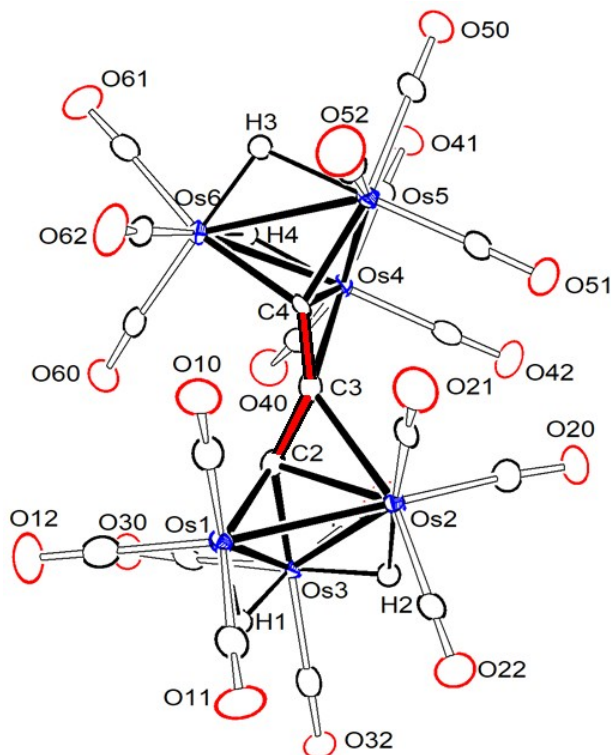


Figure 4. An ORTEP diagram of the molecular structure of $\text{Os}_3(\text{CO})_9(\mu\text{-H})_2(\mu_3\text{-}\eta^1\text{-C-C-C-}\mu_3\text{-}\eta^1)\text{Os}_3(\text{CO})_9(\mu\text{-H})_2$, **4** showing 60% thermal ellipsoid probability. Selected interatomic bond distances (Å) are as follows: $\text{Os}(1) - \text{Os}(2) = 2.7848(4)$, $\text{Os}(1) - \text{Os}(3) = 2.8821(3)$, $\text{Os}(2) - \text{Os}(3) = 2.9107(3)$, $\text{Os}(1) - \text{C}(2) = 2.070(6)$, $\text{Os}(2) - \text{C}(2) = 2.233(6)$, $\text{Os}(3) - \text{C}(2) = 2.075(6)$, $\text{Os}(2) - \text{C}(3) = 2.432(6)$, $\text{Os}(4) - \text{C}(4) = 2.226(5)$, $\text{Os}(5) - \text{C}(4) = 2.026(5)$, $\text{Os}(6) - \text{C}(4) = 2.108(6)$, $\text{Os}(4) - \text{C}(3) = 2.420(6)$, $\text{Os}(4) - \text{Os}(5) = 2.7944(3)$, $\text{Os}(4) - \text{Os}(6) = 2.8978(4)$, $\text{Os}(5) - \text{Os}(6) = 2.8930(3)$

Note added after first publication:

28th January 2019 This ESI replaces that originally uploaded on 13th March 2018 in which an incorrect CCDC number was given.

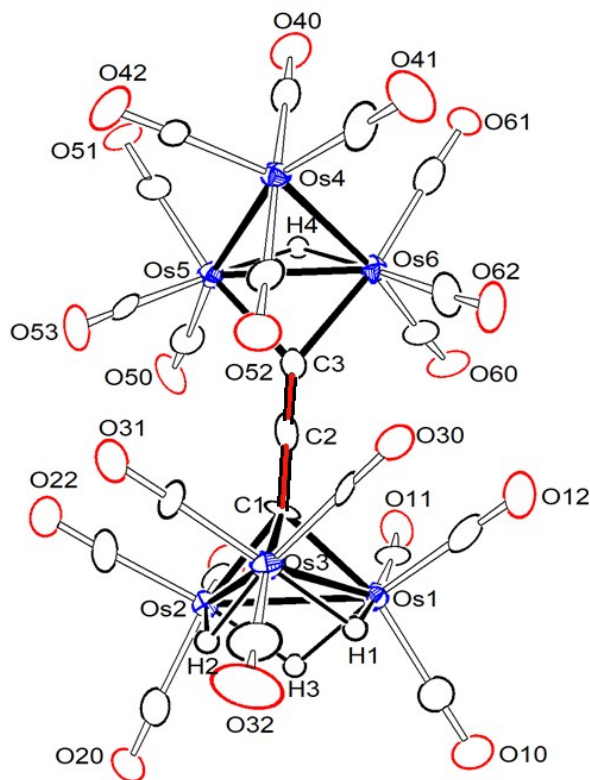


Figure 5. An ORTEP diagram of the molecular structure of $\text{Os}_3(\text{CO})_9(\mu\text{-H})_3(\mu_3\text{-}\eta^2, \text{-}\mu\text{-}\eta^2\text{-C=C=C})\text{Os}_3(\text{CO})_{10}(\mu\text{-H})$, **5** showing 60% thermal ellipsoid probability. Selected interatomic bond distances (\AA) are as follows: $\text{Os}(1) - \text{Os}(2) = 2.8652(7)$, $\text{Os}(1) - \text{Os}(3) = 2.8932(7)$, $\text{Os}(2) - \text{Os}(3) = 2.8934(7)$, $\text{Os}(1) - \text{C}(1) = 2.129(14)$, $\text{Os}(2) - \text{C}(1) = 2.148(12)$, $\text{Os}(3) - \text{C}(1) = 2.114(13)$, $\text{Os}(6) - \text{C}(3) = 2.144(13)$, $\text{Os}(5) - \text{C}(3) = 2.186(13)$, $\text{C}(1) - \text{C}(2) = 1.390(19)$, $\text{C}(2) - \text{C}(3) = 1.23(2)$, $\text{Os}(4) - \text{Os}(5) = 2.8404(7)$, $\text{Os}(4) - \text{Os}(6) = 2.8472(7)$, $\text{Os}(5) - \text{Os}(6) = 2.7868(7)$

Note added after first publication:

28th January 2019 This ESI replaces that originally uploaded on 13th March 2018 in which an incorrect CCDC number was given.

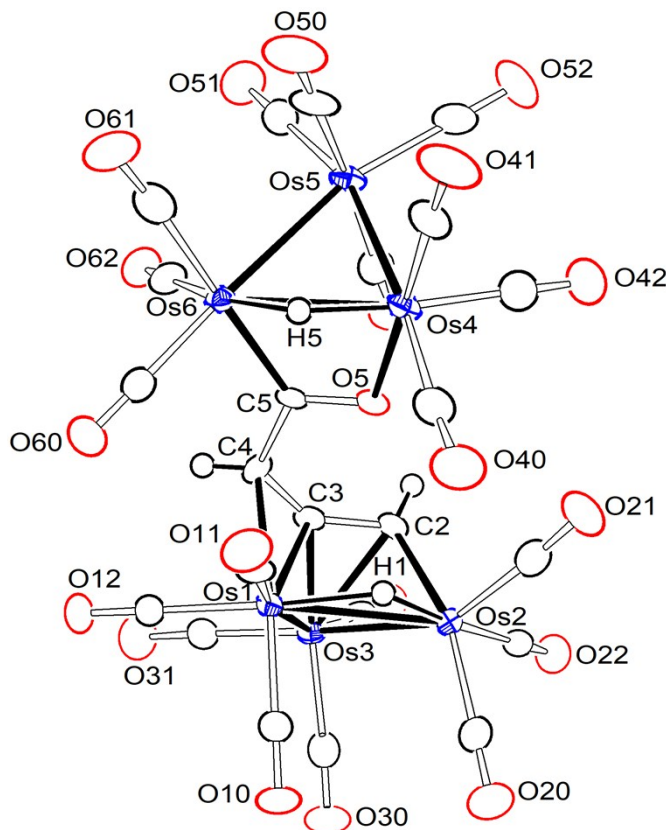
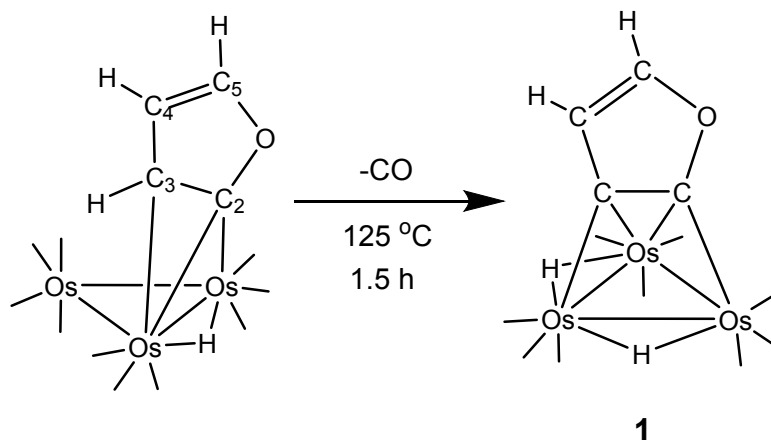


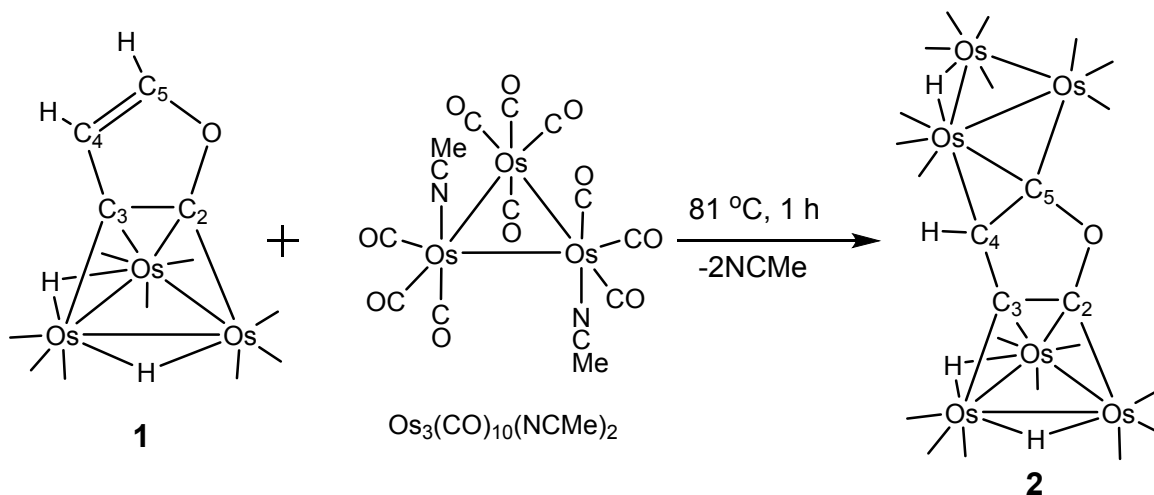
Figure 6. An ORTEP diagram of the molecular structure of $(\mu\text{-H})\text{Os}_3(\text{CO})_9(\mu_3\text{-}\eta^2\text{-CHCCHC=O-}\mu\text{-}\eta^2)\text{Os}_3(\text{CO})_{10}(\mu\text{-H})$, **6** showing 60% thermal ellipsoid probability. Selected interatomic bond distances (Å) are as follows: Os(1) – Os(2) = 3.0026(4), Os(1) – Os(3) = 2.8255(4), Os(2) – Os(3) = 2.8056(4), Os(1) – C(4) = 2.329(6), Os(1) – C(3) = 2.267(6), Os(3) – C(3) = 2.092(6), Os(3) – C(2) = 2.272(7), Os(2) – C(2) = 2.048(7), Os(4) – O(5) = 2.117(4), Os(6) – C(5) = 2.058(6), Os(4) – Os(6) = 2.9131(4), Os(4) – Os(5) = 2.8293(4), Os(5) – Os(6) = 2.8776(4), C(2) – C(3) = 1.379(9), C(3) – C(4) = 1.398(9), C(4) – C(5) = 1.476(8), C(5) – O(5) = 1.280(7)

Note added after first publication:

28th January 2019 This ESI replaces that originally uploaded on 13th March 2018 in which an incorrect CCDC number was given.



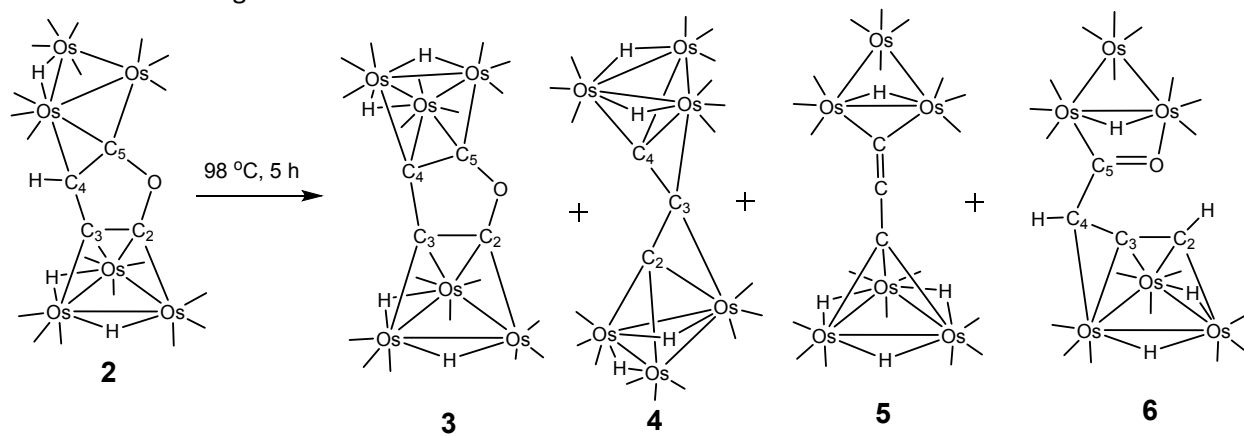
Scheme 1: A schematic of the oxidative addition of the C(3)-H bond on an Os₃ cluster



Scheme 2: A schematic of the oxidative addition of the C(5)-H bond on an Os₃ cluster followed by π -coordination.

Note added after first publication:

28th January 2019 This ESI replaces that originally uploaded on 13th March 2018 in which an incorrect CCDC number was given.

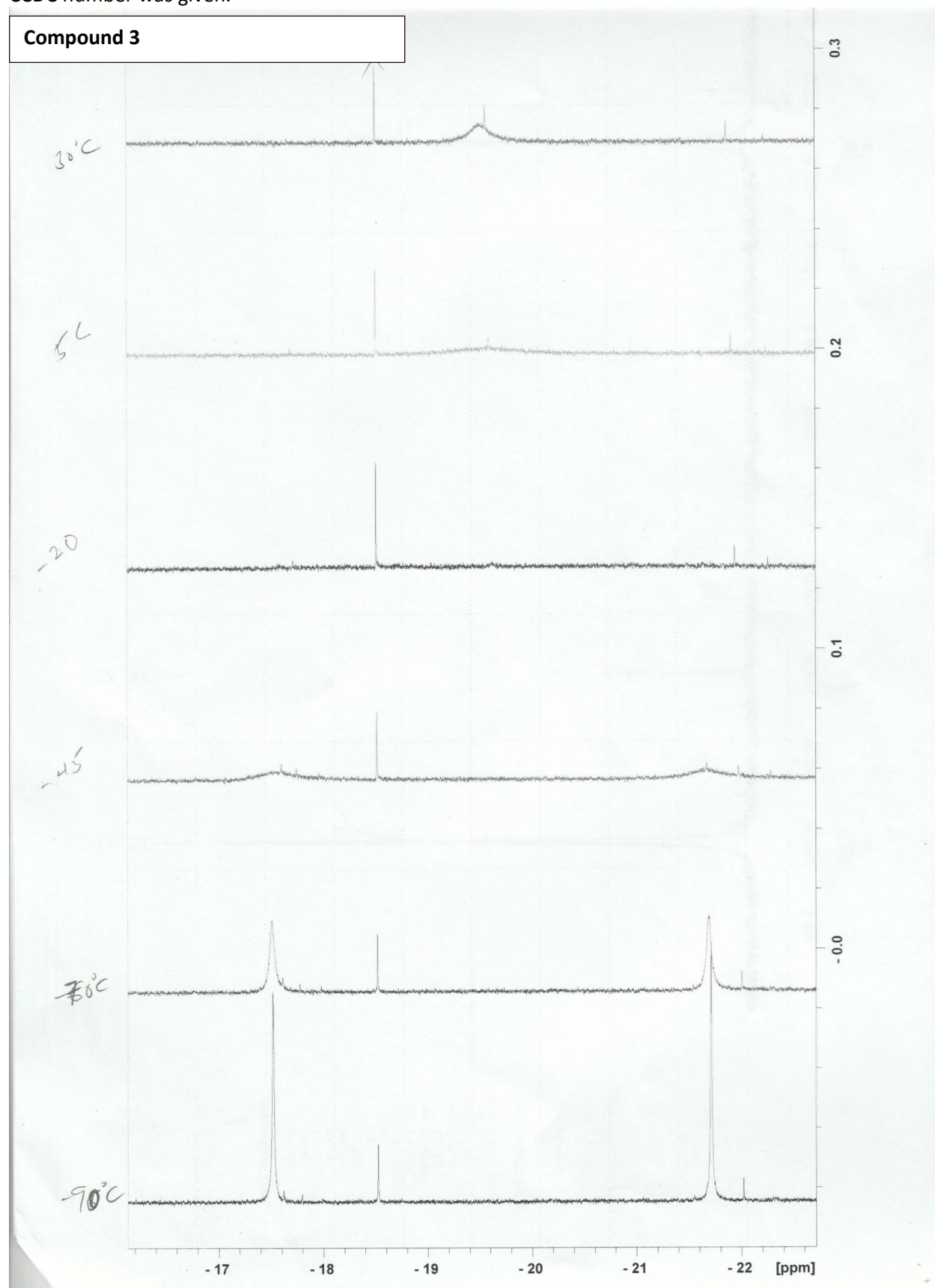


Scheme 3: Conversion of compound **2** to **3**, **4**, **5**, and **6**.

Note added after first publication:

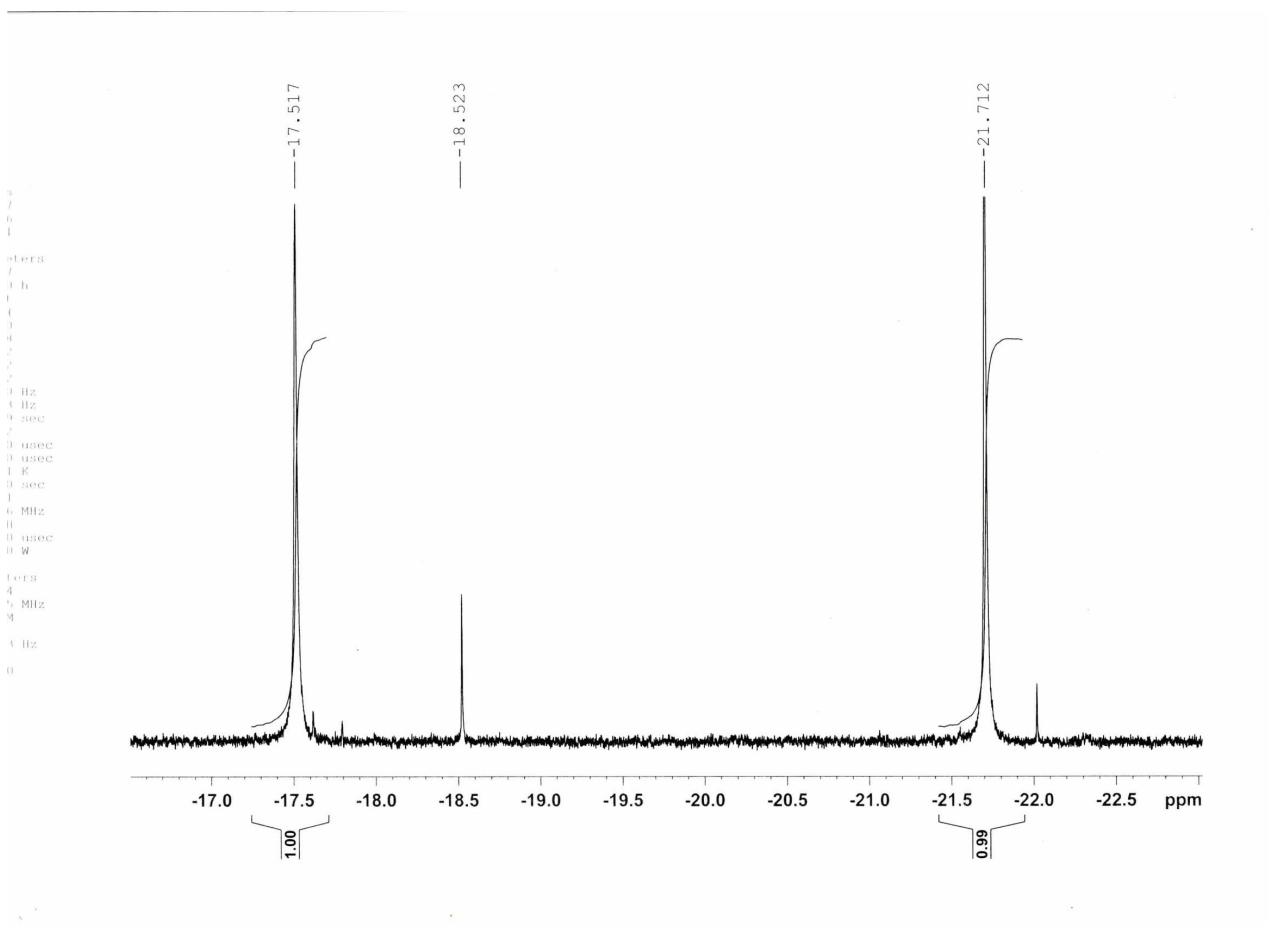
28th January 2019 This ESI replaces that originally uploaded on 13th March 2018 in which an incorrect CCDC number was given.

Compound 3



28th January 2019 This ESI replaces that originally uploaded on 13th March 2018 in which an incorrect CCDC number was given.

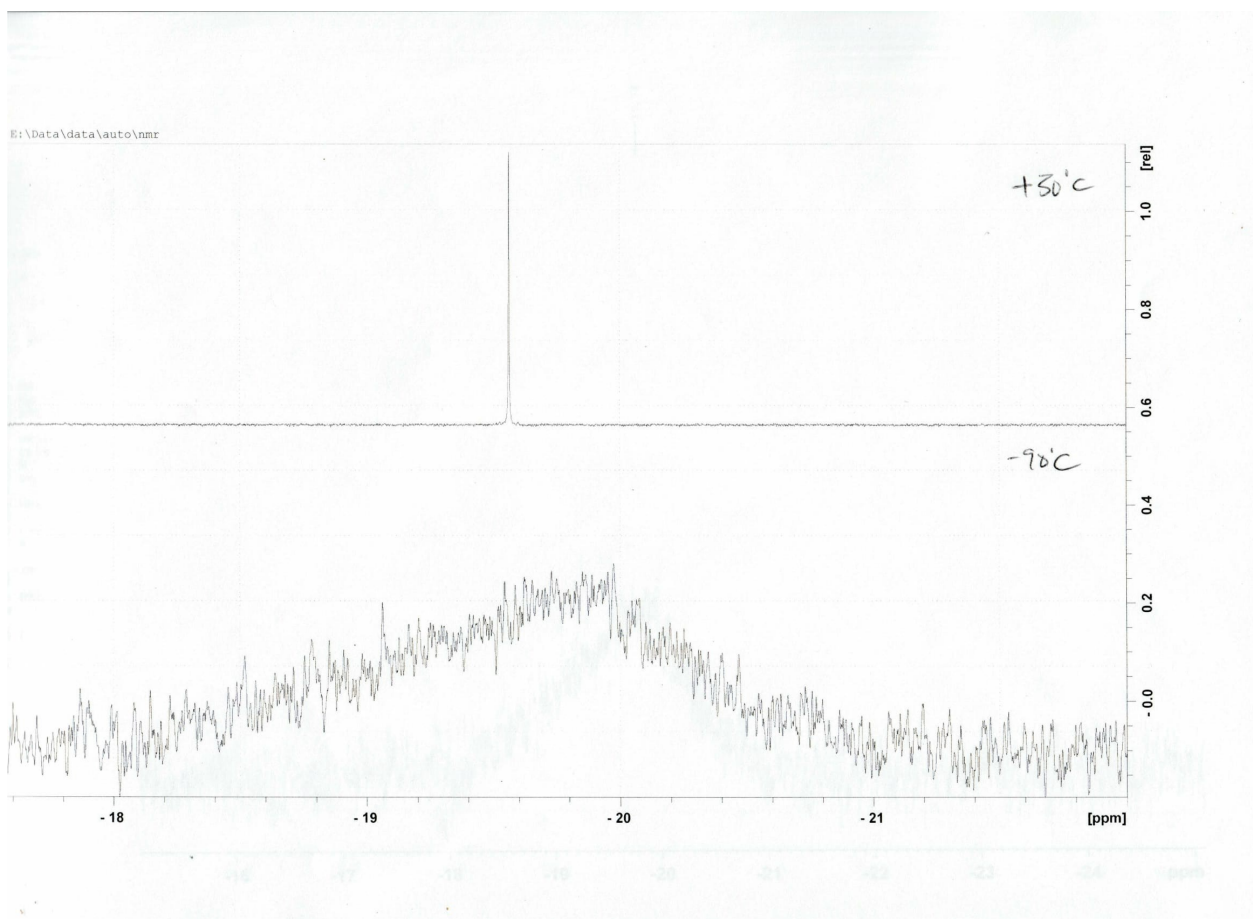
Compound 3 @ -90 °C



Note added after first publication:

28th January 2019 This ESI replaces that originally uploaded on 13th March 2018 in which an incorrect CCDC number was given.

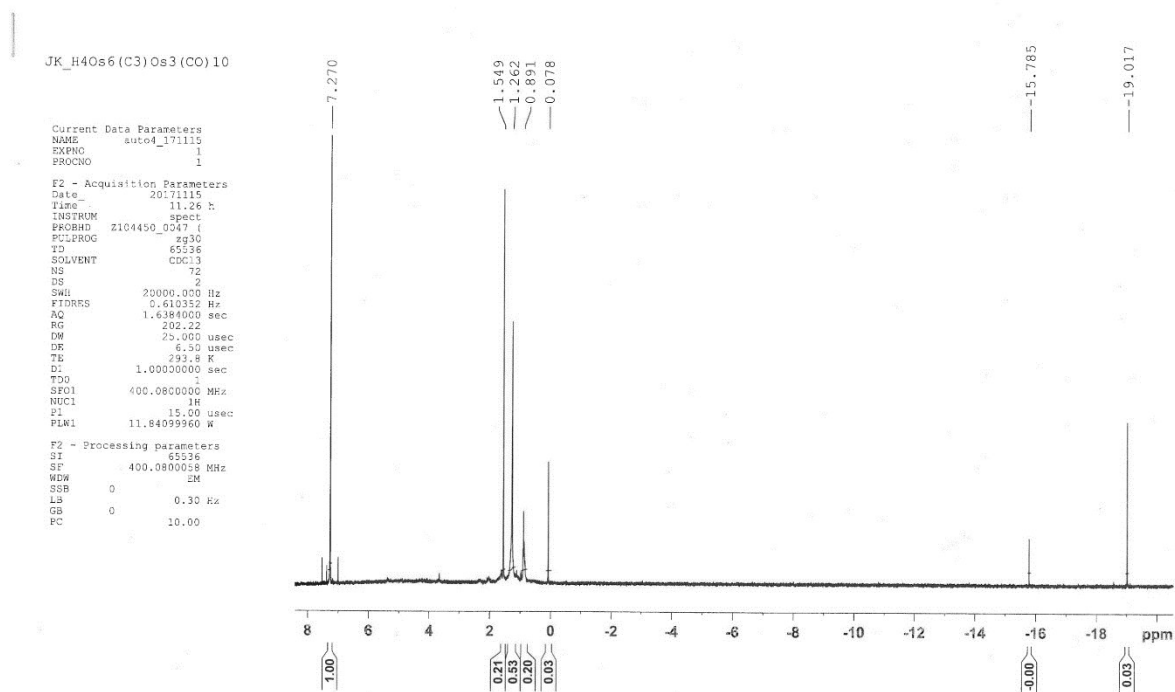
Compound 4



Note added after first publication:

28th January 2019 This ESI replaces that originally uploaded on 13th March 2018 in which an incorrect CCDC number was given.

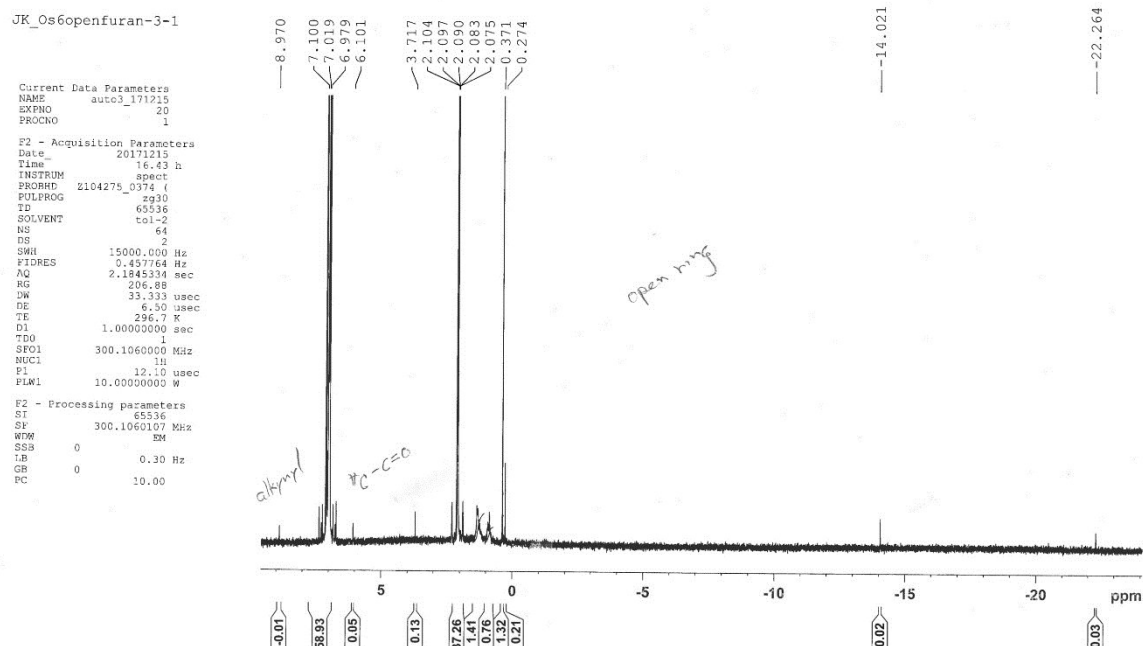
Compound 5



Compound 6

Note added after first publication:

28th January 2019 This ESI replaces that originally uploaded on 13th March 2018 in which an incorrect CCDC number was given.



References

- [1] D. Braga, F. Grepioni, E. Parisini, B. F. G. Johnson, C. M. Martin, J. G. M. Nairn, J. Lewis, M. Martinelli, *J. Chem. Soc.-Dalton Trans.* **1993**, 1891-1895.
- [2] D. Himmelreich, G. Muller, *J. Organomet. Chem.* **1985**, 297, 341-348.
- [3] *SAINT+*, Version 6.2a; Bruker Analytical X-ray Systems, Inc.: Madison, WI 2001.
- [4] G. M. Sheldrick, *SHELXTL*, Version 6.1 ed., Bruker Analytical X-ray Systems, Inc., Madison, WI, **1997**.
- [5] *APEX3 Version 2016.5-0 and SAINT Version 8.37A.*, Bruker AXS, Inc.: Madison, WI, USA.
- [6] *SADABS 2016/2*; Bruker Analytical X-ray Systems, Inc.: Madison, WI, USA, 2016.
- [7] *Cell Now Version 2008/4*. Bruker Analytical X-ray Systems, Inc., Madison, Wisconsin, USA, 2016

Note added after first publication:

28th January 2019 This ESI replaces that originally uploaded on 13th March 2018 in which an incorrect CCDC number was given.

[8] TWINABS Version 2012/1. Bruker Analytical X-ray Systems, Inc., Madison, Wisconsin, USA, 2016

[9] SHELXT: G. M. Sheldrick. *Acta Cryst.* **2015**, *A71*, 3-8.

[10] SHELXL: G. M. Sheldrick. *Acta Cryst.* **2015**, *C71*, 3-8.

[11] OLEX2: O. V. Dolomanov, L. J. Bourhis, R. J. Gildea, J. A. K. Howard and H. Puschmann. *J. Appl. Cryst.* **2009**, *42*, 339-341.